



# Fischer–Tropsch Synthesis: Reaction mechanisms for iron catalysts<sup>☆</sup>

Burtron H. Davis<sup>\*</sup>

Center for Applied Energy Research, University of Kentucky, 2540 Research Park Drive, Lexington, KY 40324, USA

## ARTICLE INFO

### Article history:

Available online 29 April 2008

### Keywords:

Iron catalyst  
Fischer–Tropsch synthesis  
Reaction mechanism  
Catalyst structure

## ABSTRACT

The reaction mechanism for the Fischer–Tropsch synthesis with iron catalysts under low-temperature conditions is described. Our data are considered to support an oxygenate intermediate. The structure of the chain initiating species is considered to be, or closely resembles, the formate species responsible of the water–gas shift reaction. Chain propagation is considered to involve a different species that is either CO or a species derived from CO. The growing chain is considered to lose the final oxygen during the chain termination step. The structure of the stable low-temperature iron catalyst is considered to consist of a core that is Fe<sub>3</sub>O<sub>4</sub> with the core surrounded by a layer of iron carbide. The data show that iron carbide is the active phase and that there is a synergistic interaction between the alkali and structural promoter that maintains an adequate iron carbide layer.

© 2008 Elsevier B.V. All rights reserved.

## 1. Introduction

While good data are matters of fact and stand the test of time, reaction mechanisms are more a matter of opinion and are subject to change. This is certainly the situation with the mechanism for the Fischer–Tropsch reaction. In the following we shall briefly consider the development of the ideas for the mechanism of the Fischer–Tropsch Synthesis (FTS). The development will be followed along two paths. First, the views of the reaction will be outlined and then the proposals of the active catalyst will be developed.

While many reports do not make a distinction between “low and high” temperature operations, it is essential that this should be done. Thus, this review will concentrate primarily on low-temperature FTS. There are significant similarities between low and high temperature FTS using an iron catalyst, and many important differences.

## 2. Period following introduction (discovery to 1940)

Fischer is usually attributed to be the first to advance the carbide mechanism for the Fischer–Tropsch Synthesis (FTS). However, in his book Fischer described work that predated their publications in scientific journals, and he offered a number of mechanism possibilities for the reaction. These were [1]:

1. Formation of formaldehyde in contact with metallic hydrogen carriers [ $2\text{CH}_2\text{O} = \text{CO}_2 + \text{CH}_4$ ].

2. Modification of reaction 1—in the presence of bases or salts the following is possible: [ $2\text{CH}_2\text{O} = \text{CH}_3\text{OH} + \text{CO}$ ].
3. Synthesis by condensation of aldehydes—higher alcohols analogous to aldol condensation as is known to be especially favored by the presence of alkali.
4. Synthesis by CO addition to alcohols. Just as CO combines with water to produce formic acid, it might unite with methanol to give acetic acid and, by analogy, higher alcohols.
5. Synthesis of higher alcohols by dehydration [ $\text{C}_n\text{H}_{2n+1}\text{ONa} + \text{C}_m\text{H}_{2m+1}\text{OH} = \text{C}_{n+m}\text{H}_{2(n+m)+1}\text{OH} + \text{NaOH}$ ].
6. Other possibilities considered by Fischer included:
  - a. Without wishing to decide as yet in favor of any one of the suggested interpretations, since several modes of formation may run concurrently, synthesis by addition of CO to alcohols seems to be the most lucid and consistent.
  - b. An explanation involving the reduction of CO down to a  $\text{CH}_2$ -group, the union of such groups to olefins, and the hydration to alcohols seems hardly probable...we have found practically no liquid hydrocarbons in these reactions.

Thus, to explain his early results where oxygenates were the dominant products, Fischer did not support a carbide mechanism; his support for that mechanism only came after results showed that hydrocarbons could be the dominant products. Thus, by 1926 Fischer and Tropsch [2] suggested that the carbide mechanism whereby carbides that were formed from the synthesis gas were then hydrogenated to methylene groups. These methylene groups could polymerize to form hydrocarbon chains that desorb from the surface as saturated and unsaturated hydrocarbons.

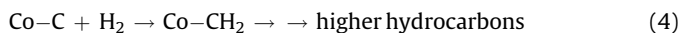
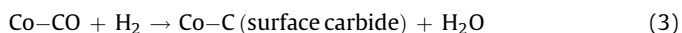
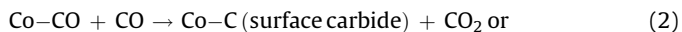
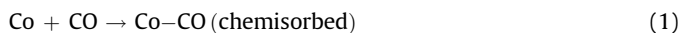
At the end of this period a more detailed carbide mechanism was introduced by Craxford and Rideal [3]. In this mechanism, the CO is

<sup>☆</sup> This forms part of the plenary lecture delivered in the symposium.

<sup>\*</sup> Tel.: +1 859 257 0251.

E-mail address: [davis@caer.uky.edu](mailto:davis@caer.uky.edu).

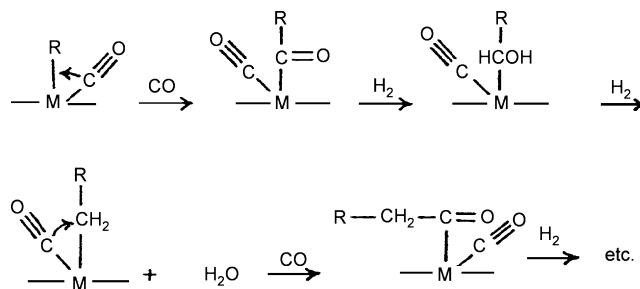
adsorbed on the surface and dissociates, in the presence of hydrogen, by forming water or CO<sub>2</sub> which rapidly desorbs and chemisorbed carbon is formed. The carbon is subsequently hydrogenated to form chemisorbed CH<sub>2</sub> which oligomerizes to produce higher carbon number hydrocarbons by the reactions shown below.



The authors, in order to elucidate the reaction mechanisms, studied the conversion of *para*- to *ortho*-hydrogen when starting with *para*-hydrogen/carbon monoxide mixtures and using a cobalt catalyst. They found that the *para*- to *ortho*- conversion did not occur to any extent when the reaction was conducted at 200 °C, but did occur when no reaction was occurring or when the product was essentially methane only. The authors concluded that no appreciable amount of atomic hydrogen was present during normal synthesis. They postulated that the surface of cobalt was essentially completely covered by cobalt carbide during normal synthesis and this inhibited the dissociation of hydrogen, as shown in the above equations. Chain growth was postulated to continue until split by hydrogen. They indicated that there was a pseudo-equilibrium that existed between methylene formation/polymerization and hydrogenolysis. Later studies show that hydrogen–deuterium exchange does occur and this calls into question the lack of *o*-*p*-hydrogen exchange.

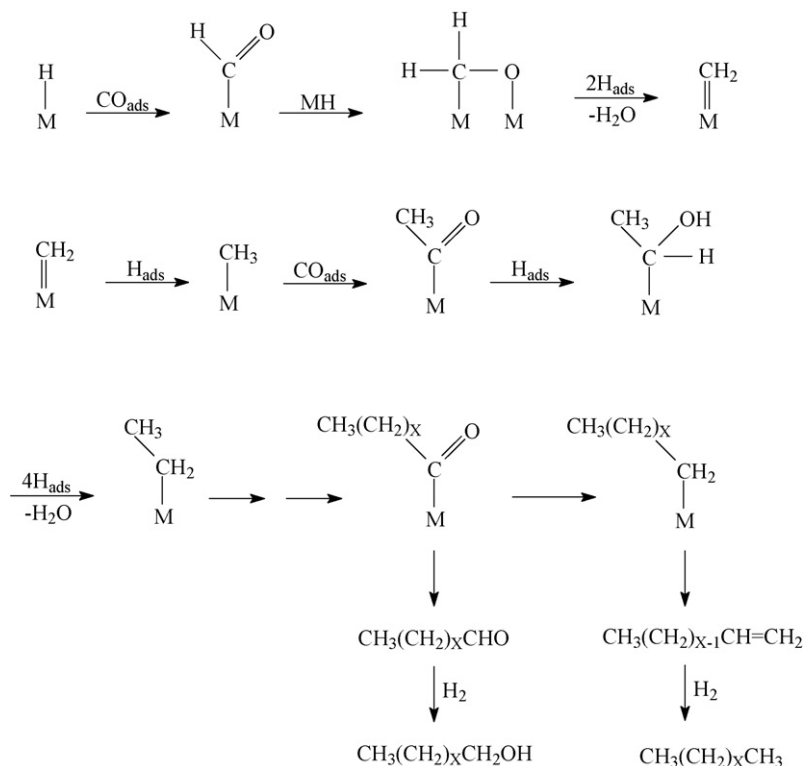
### 3. The oxygenate mechanism (1940–1970)

Mechanism work on the Fischer–Tropsch synthesis was nearly eliminated during the WWII years. The commercial operations, using a cobalt-based catalyst, continued during the war years but



Scheme 1.

building new plants was terminated in Germany before 1940. By 1945 there was a perception that western countries were facing a critical shortage of petroleum. This led Percival “Dobbie” Keith to form Hydrocarbon Research Inc. (HRI) with the intention of commercializing the Fischer–Tropsch process in the US. Keith was the Vice President at Kellogg when the war began. Kellogg became involved in the research to separate uranium isotopes and, not wanting the company to be connected to a failure should the process not work, established a subsidiary, Kelex, to carry out the work for the US government. Keith headed Kelex and directed uranium isotope separation research efforts. Keith was responsible for building and starting the operations of the Oak Ridge National Laboratory and the secret uranium isotope separation plant. Toward the end of the war, Keith became interested in the Fischer–Tropsch process and formed HRI because of this interest. He and Paul Emmett, also involved in the Manhattan Project, were at the same location and frequently had lunch together. During these lunches, the Fischer–Tropsch process was a main topic of discussion [4]. Keith made progress and built a commercial scale plant (ca. 8,000 bbl/d) in Texas. Unfortunately, just as the plant was approaching the production of the design capacity of hydrocarbon



Scheme 2.

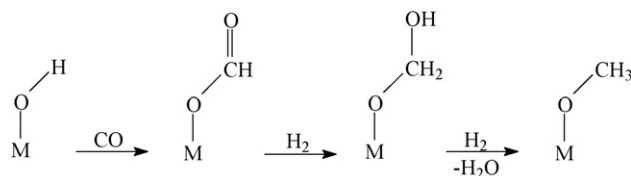
fuels, the rise in the price of the natural gas feedstock caused the plant to be shut down.

Near the end of the war, Emmett joined the Mellon Institution and undertook studies of the Fischer–Tropsch synthesis. He was fortunate that his work on the Manhattan Project made him aware of the use of radioisotopes and provided connections at Oak Ridge so that he could obtain some of the initial supplies of  $^{14}\text{C}$ . This enabled him to conduct pioneering studies employing  $^{14}\text{C}$ -tracers in the study of FTS. Using  $^{14}\text{C}$  he was able to show that the hydrogenation of iron carbide labeled with  $^{14}\text{C}$  was not the dominant source of the hydrocarbons and thereby requiring their formation by the reaction of CO with  $\text{H}_2$  [5]. This result supported his earlier calculations showing that the hydrogenation of iron carbide to form hydrocarbons was not the reaction pathway [6].

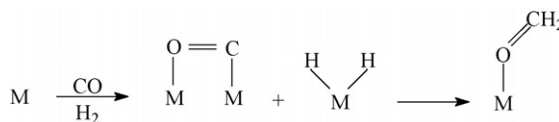
The work of Emmett and coworkers, combined with the work at the US Bureau of Mines, led to the wide spread acceptance of the oxygenate reaction mechanism for FTS [7]. The US Bureau was funded with about ninety million dollars during a 10-year period for both direct and indirect coal liquefaction. The funding included the construction and operation of a 70 bbl/d pilot plant for FT synthesis. The technical work was headed by H. H. Storch and he was joined in 1945 by Robert B. Anderson. The Bureau team conducted extensive research both on the scientific and the development stages. Some important work included:

- 1944 R. B. Anderson and S. Weller join and Anderson to FT Catalyst Testing Section in 1945.
- FTS in small pilot plants at Bruceton initially under J. H. Crowell, followed by H. E. Benson in 1947 and J. H. Field in 1948.
- Benson and Field were the major contributors to the development of the oil recirculation and the hot-gas-recycle processes.
- M. D. Schlesinger led studies of FTS in slurry and fluidized-bed reactors.

The early British effort in FT was curtailed by WWII. However, British Gas made a significant effort following the end of WWII and took advantage of the background knowledge they obtained from captured German documents and from the Allies interviews of Germans who worked on FT synthesis. The British workers concluded that, “These observations, together with the evidence previously available, strongly suggest that alcohols are the true primary products of the Fischer–Tropsch synthesis on both cobalt and iron catalysts...” [8].



Scheme 3.



Scheme 4.

Wender and coworkers [9] conducted work on hydroformylation and at the end of a short note offered a mechanism for the FT reaction as shown in Scheme 1.

The authors noted that the scheme may encounter steric difficulties unless the surface is sparsely occupied but that insertion of CO from a neighboring metal atom may occur.

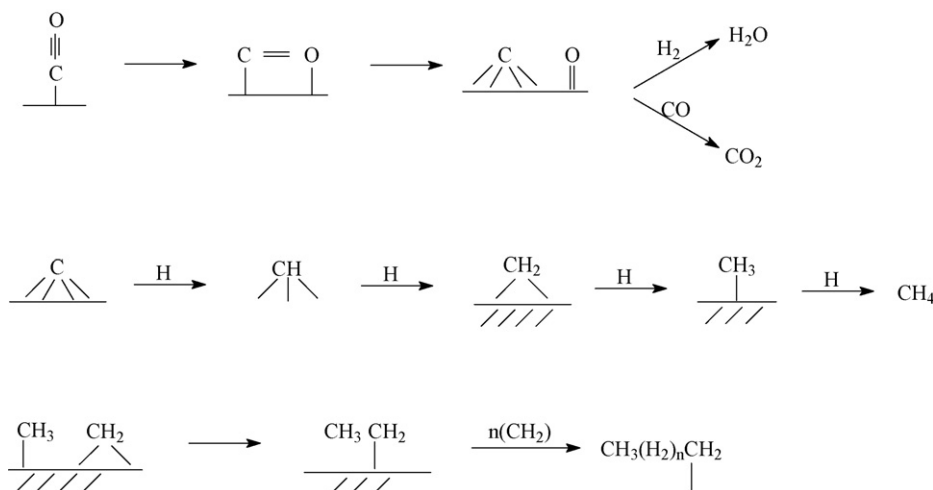
The CO insertion mechanism outlined in Scheme 2 has been identified as the Pichler–Schulz mechanism [10]. This mechanism differs from the surface carbide mechanism in the pathway leading to the formation of the adsorbed methylene group and then resembles the CO insertion mechanism offered by Wender and coworkers. The reaction mechanism is shown in Scheme 2.

A unique mechanism was advanced by Deluzarche et al. [11] wherein they propose that CO inserts between the O and H bond of an adsorbed OH group, as shown in Scheme 3.

An even more unique mechanism was advanced by Sapienza et al. [12] in which adsorbed CO is hydrogenated so that the oxygen is bonded to the surface as shown in Scheme 4.

#### 4. The surface carbide mechanism (1970 to present)

With the advent of the surface science instrumentation, the view shifted from the oxygenate to once again the carbide mechanism. A reason for this was the observations made using surface science instruments that show essentially the absence of



Scheme 5.

oxygen on the catalyst surface but an abundance of carbon. This led to the view that it was a surface, or near surface, metal carbide that was the initial surface species in the formation of carbenes. Maitlis indicated that this mechanism should be named the Fischer–Tropsch–Brady–Pettit–Biloen–Sachtler mechanism.

Pettit and coworkers utilized the addition of  $\text{CH}_2\text{N}_2$  and obtained results that were interpreted to support a mechanism that was a polymerization of adsorbed methylene ( $\text{CH}_2$ ) groups [13]. When initiating with syngas, Pettit's group would consider the methylene groups to be formed by the addition of hydrogen to adsorb carbon that was produced by the dissociation of CO. This mechanism received support from the results obtained by Biloen, Sachtler and coworkers using catalysts covered by  $^{13}\text{C}$ . Thus, these results are consistent with the mechanism shown in Scheme 5.

Brady and Pettit [13] utilized their data where they employed  $^{13}\text{C}$ -tracer and compared the data that they would obtain for three mechanisms: chain propagation by methylene, condensation of methylene groups with elimination of water as required by the work of Storch et al. [7] and Emmett and coworkers [4,5], and the scheme wherein CO is inserted into the metal–alkyl group as advanced by, for example, Pichler and Schulz [10]. The only mechanism that was in agreement with the data of Pettit's group was the mechanism where chain growth was due to polymerization of methylene groups.

Ritschel and Vielstich [14] dissolved the used Fischer–Tropsch catalysts in HCl and found that the gaseous hydrocarbons produced during dissolution and the ones produced during the FT synthesis were qualitatively similar. These results were considered to support the surface carbide mechanism [15].

Indirect evidence for the surface carbide mechanism involving methylene was obtained by “scavenging” reactions with an added compound. Thus, Bell [16] added cyclohexene to the syngas under synthesis conditions over a ruthenium catalyst and the formation of norcarane along with alkyl cyclohexenes was considered to be the result of the added compound reacting with surface  $\text{CH}_2$  groups. Similar conclusions were reached by other investigators [17–19].

## 5. Our return to the oxygenate mechanism

We returned to the approach used by Emmett and coworkers of adding a  $^{14}\text{C}$ -labeled compound during synthesis. In these studies we utilized a CSTR so that the changing concentrations of labeled compound down the bed of a fixed-bed reactor were eliminated. The initial results were obtained by adding  $^{14}\text{C}$ -labeled ethanol. The results for the lower carbon number compounds were essentially the same as obtained by Emmett and coworkers with the radioactivity per mole for the  $\text{C}_2$ – $\text{C}_4$  products being constant. This constant activity per mole was consistent with the ethanol initiating chain growth and not participating in chain growth. However, the activity of the higher carbon number compounds decreased with an increasing carbon number. Initially this was explained by a two-chain growth mechanism wherein the one chain growth followed the pathway of the adsorbed ethanol, and therefore, produced the  $^{14}\text{C}$ -labeled higher carbon number compounds. The other chain growth produced only alkanes and the adsorbed alcohol did not contribute to this chain's growth. Thus, the initial results were interpreted using a two-chain growth mechanism that had been proposed by several earlier workers.

Further studies clearly showed that the decrease in the  $^{14}\text{C}$ -activity was due to the accumulation of heavier reaction products in the CSTR and that these diluted the products made during the period when the  $^{14}\text{C}$ -labeled compound was added. Subsequent work with deuterium isotopic tracers confirmed that this was the case.

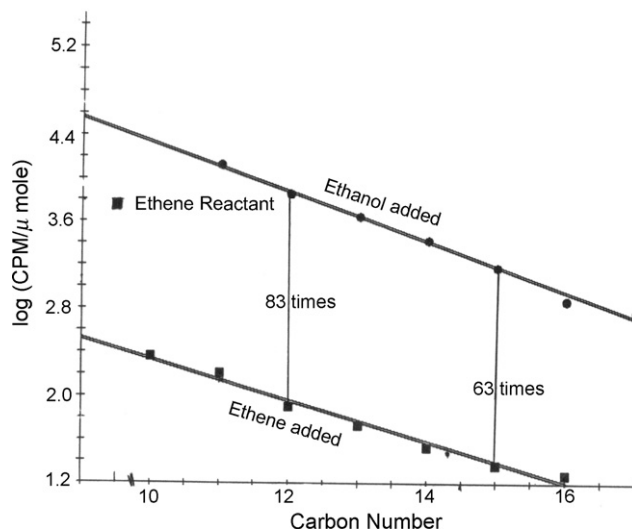


Fig. 1. The radioactivity in the products produced when  $^{14}\text{C}$ -labeled ethanol (●) and ethene (■) were added to the synthesis gas during FT synthesis.

With the iron catalyst the addition of  $^{14}\text{C}$ -labeled ethanol and ethene derived from the ethanol clearly showed that the alcohol incorporated at least 50–100 times as much as the alkene (Fig. 1). Several carbon number alkenes and alcohols labeled with  $^{14}\text{C}$  have been added so that the labeled compound is not a dominant carbon species (the labeled compound is about 2% of the total carbon added during the synthesis with labeled compound). In spite of this, the need to add sufficient  $^{14}\text{C}$  to be able to detect accurately the amount of label in the many compounds that are produced caused the labeled higher molecular weight compounds to be present in as large, or even larger, amount as that produced during synthesis.

A schematic of the results for the addition of the  $\text{C}_2$ – $\text{C}_{10}$  alcohols and alkenes is shown in Fig. 2. The data show that ethene can compete with the CO for catalytic sites and undergoes significant hydrogenation in addition to initiating growing chains. This was shown since at least 60% of the added ethene was hydrogenated to ethane during the addition of the  $^{14}\text{C}$ -labeled ethene. On the other hand, the  $^{14}\text{C}$ -labeled 1-pentene did not hydrogenate to a measurable level even though some of the added alkene adsorbed and initiated some chain growth. In the case of  $^{14}\text{C}$ -labeled 1-decene,

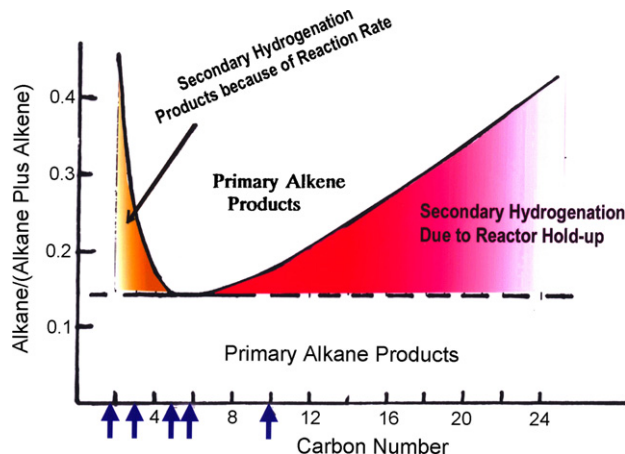


Fig. 2. Schematic for the alkene/(alkene + alkane) fraction versus carbon number for FT synthesis [(↑) indicates carbon numbers where  $^{14}\text{C}$ -labeled alkene or alcohol was added].

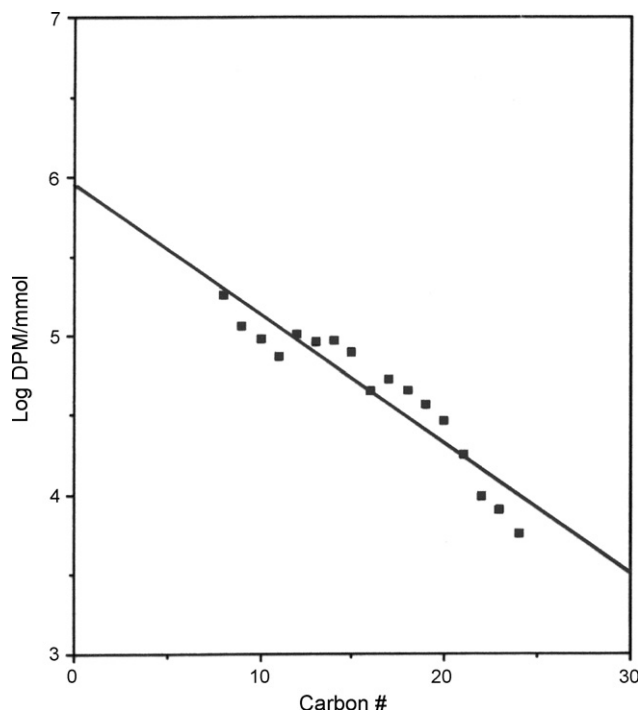


Fig. 3. Radioactivity versus the carbon number for the alkane fraction produced during FT synthesis when  $^{14}\text{C}$ -labeled ethene was added to the synthesis gas.

at least as much of the added alkene was hydrogenated as initiated chain growth. These data clearly show the reactor hold-up and the competitive chemisorption impacts the data generated in tracer studies and that these factors must be taken into account when developing reaction mechanisms. The impact of the reactor on the dilution of the higher carbon number products is illustrated by the data comparing the results obtained when  $^{14}\text{C}$ -labeled 1-pentanol is added to the synthesis gas. The volume of liquid held-up in the fixed-bed reactor is much less than the volume of liquid in the CSTR; hence, the decline in radioactivity with carbon number is much less for the fixed-bed reactor than it is for the CSTR. When the reaction is carried out in a fixed-bed reactor operating at atmospheric pressure the radioactivity in the products is essentially constant from carbon number 10 to 22. Thus, while the CSTR has the advantage that the conversion is conducted with a constant gas phase composition and conversion level, the reactor has a large reserve of liquid products which dilute the products.

The impact of the dilution by products was demonstrated by separating the alkane and the alkene fractions from the products collected when adding  $^{14}\text{C}$ -labeled ethanol using silica gel chromatography. The  $^{14}\text{C}$  per mole for each carbon number for the alkane fraction showed the decline that was obtained for the total sample (Fig. 3). However, when the  $^{14}\text{C}$ -label of the alkene fraction was plotted versus the carbon number a straight line with no slope was obtained (Fig. 4); thus, the radioactivity per mole of alkene was the same for this carbon number range. The accumulated products had been retained in the reactor long enough for the initial alkene products to be hydrogenated to the alkane. Thus, the alkanes that were formed during the addition of the  $^{14}\text{C}$ -labeled compound were diluted by the accumulated alkanes and this accounted for the decrease in  $^{14}\text{C}$ -activity with increasing carbon number. However, the alkenes were hydrogenated rapidly enough that little alkene accumulation had occurred and the alkenes formed during the  $^{14}\text{C}$ -labeled ethanol addition were not diluted by accumulated products showing that the added  $^{14}\text{C}$ -labeled ethanol only initiated chain growth.

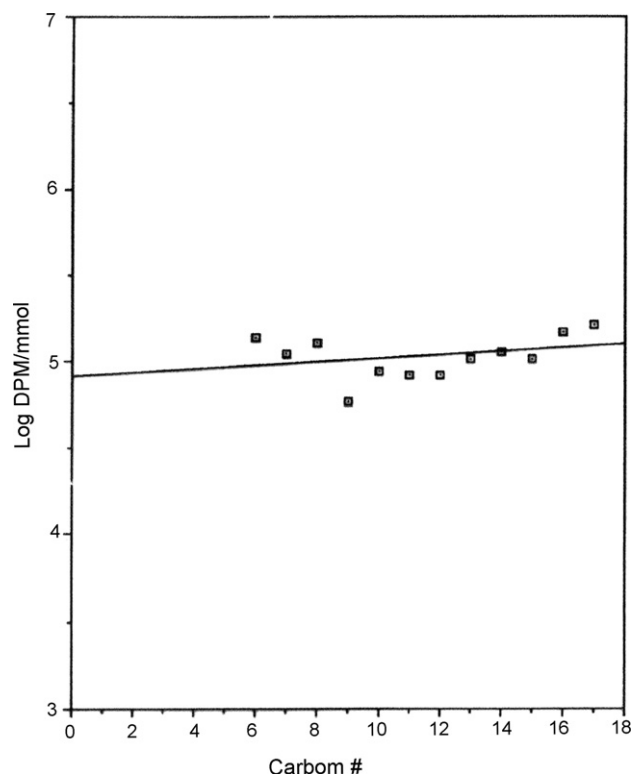


Fig. 4. Radioactivity versus the carbon number for the alkene fraction produced during FT synthesis when  $^{14}\text{C}$ -labeled ethene was added to the synthesis gas.

Emmett and coworkers converted a number of  $^{14}\text{C}$ -labeled primary and secondary alcohols. As shown in Fig. 5, the primary alcohols produced essentially normal alkanes whereas the secondary alcohols produced mostly the *iso*-alkanes. Emmett and

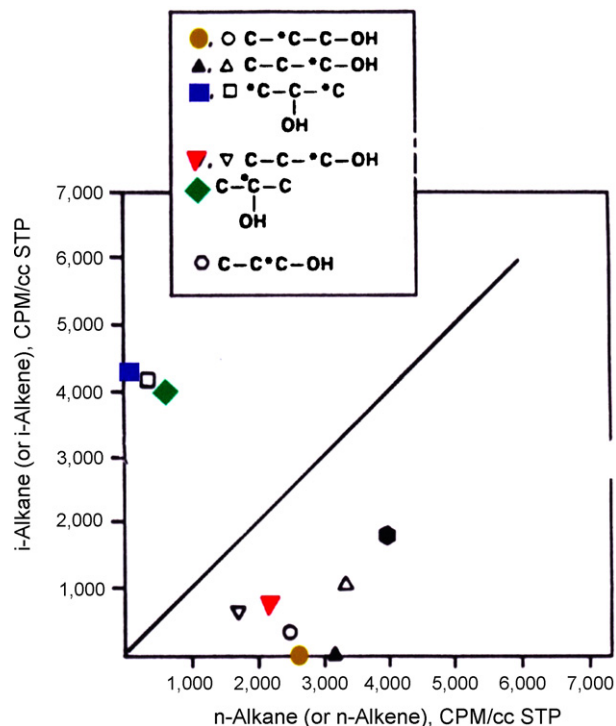
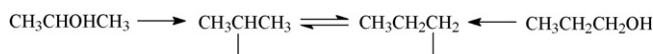


Fig. 5. The radioactivity in the *iso*-alkane and *n*-alkane formed when adding either a normal or *iso*-alcohol during FT synthesis (data from Emmett and coworkers and our lab).





Scheme 6.

coworkers did not emphasize this fact in their publications. We have repeated several of these runs with the advantage that we can analyze the products in more detail using gas and liquid chromatography. Our results are in excellent agreement with those obtained earlier by Emmett and coworkers. In the conversion of  $^{14}\text{C}$ -labeled 1- and 2-propanol during the FTS reaction, we note that 1-propanol is incorporated to a much greater extent than 2-propanol. Furthermore, the 1-propanol produces mainly  $^{14}\text{C}$ -labeled *n*-alkanes and *n*-alkenes whereas 2-propanol produces predominantly  $^{14}\text{C}$ -labeled *iso*-alkanes and *iso*-alkenes. These observations have a significant impact upon the permissible reaction mechanisms provided readsorbed alcohols follow the same reaction pathway that the FTS reaction does. If the oxygen is lost from the alcohols to form an adsorbed alkyl group, the following surface reaction is expected to make a common intermediate for each alcohol, and this would, therefore, lead to the same product distribution, which is not observed (Scheme 6).

Only if the equilibration between the 1- and 2-adsorbed alkyl groups does not occur can the two alcohols produce different products, and this seems very unlikely. Therefore, these results strongly support a reaction mechanism whereby the oxygen remains attached to the carbon until the next carbon–carbon bond is established by the reaction with adsorbed CO.

Very strong support for an oxygenate mechanism for the iron catalysts comes from experiments in which  $^{14}\text{CO}_2$  was added to the synthesis gas, with the carbon in  $\text{CO}_2$  representing only 2% of the total carbon added. Under reaction conditions where the carbon is predominantly in CO the conversion of  $\text{CO}_2$  is very low. The incorporation of  $^{14}\text{C}$  in the  $\text{CO}_2$ , however, permits us to follow the fate of the small amount of carbon in the hydrocarbons that is derived from  $\text{CO}_2$ . The important result is that while the reverse WGS occurs only to a slight extent, it does occur to produce CO with a low concentration of  $^{14}\text{C}$  (Fig. 6). If only CO initiated chain growth and was responsible for the chain propagation the methane and methanol should have the same radioactivity as the CO and the radioactivity of each carbon number compound, *n*, should be *n* times the radioactivity of the CO. The radioactivity of the products produced with a catalyst used in LaPorte, Texas pilot plant Run 2 is

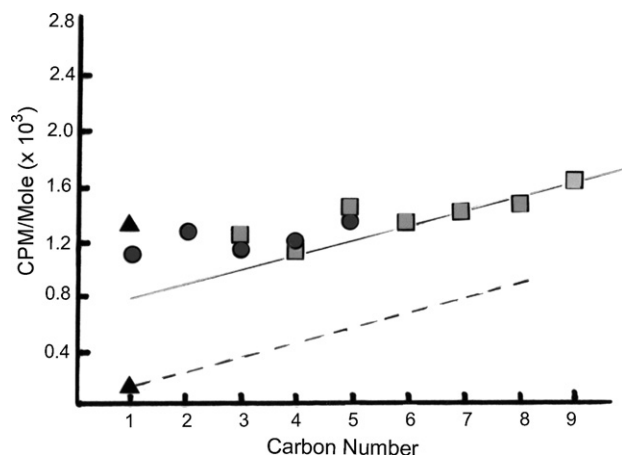
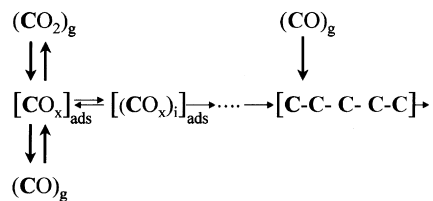


Fig. 6. Radioactivity versus carbon number for hydrocarbons formed during FT synthesis during addition of  $^{14}\text{CO}_2$  to the synthesis gas [activity for gas analysis (●) and liquid analysis (■); (---) activity expected if initiation and propagation was by CO only].



Scheme 7.

shown in Fig. 6. This catalyst contained 12.2 wt.% Cu and about 0.1% K and this provides significant WGS activity. The data in Fig. 6 make it clear that the products in the  $\text{C}_1$ – $\text{C}_9$  range contained much more radioactivity than they could have if both initiation and propagation had involved only CO (as shown by the broken line in Fig. 6). An important second observation is that the radioactivity of the  $\text{C}_2$ – $\text{C}_9$  products are not *n* times that of the  $\text{C}_1$  product. These data, therefore, require that the initiator of chain growth be different from that of the chain propagation species. It is important to recognize that the data in Fig. 6 applies only to the conversion of the  $^{14}\text{C}$ -labeled components. Thus, while the radioactivity of the  $\text{C}_1$  compounds is about half of that of the radioactivity of the  $\text{CO}_2$ , this does not mean that half of the labeled and unlabeled  $\text{C}_1$  compounds are derived from  $\text{CO}_2$ . The data shown in Fig. 6 are consistent with a mechanism that utilizes a surface species that is involved in the WGS reaction initiating the FT synthesis and that the propagation steps involve the addition of CO, or a surface species derived from CO. The important conclusion from this data is that different surface chemical species are involved for chain initiation and for chain propagation; this is illustrated in Scheme 7.

One of the mechanistic uncertainties for the results described above is that it was not possible to determine whether the  $^{14}\text{C}$ -labeled species are added in the initiation or the termination step. To define this a run was made in which  $^{14}\text{C}$ -labeled ethene, ethanol or propanol was added to the syngas [20]. The products were separated into the alkane and alkene fractions. The liquid alkenes were then oxidized to selectively convert the terminal carbon of the alkene to  $\text{CO}_2$ . The oxidation of  $^{14}\text{C}$ -1-hexene showed that the oxidation did selectively convert the terminal position of the alkene to  $\text{CO}_2$ . For the run with  $^{14}\text{C}$ -labeled ethene, the terminal position of the alkene should have half the activity of the ethene if the mechanism involved the added alkene in the termination step. However, the radioactivity in the terminal position of the alkenes formed during the addition of  $^{14}\text{C}$ -ethene did not, within experimental error, contain the  $^{14}\text{C}$ -label. A similar result was obtained for the addition of the alcohols. Thus, the conclusion is that the added alkene or alcohol did not function to terminate the chain but rather to serve as the initiator for chain growth.

Similar conclusions were reached by Emmett and coworkers who determined the radioactivity in the  $\text{C}_3$  fraction from the conversion of ethanol labeled in the 1- and 2-position. When the ethanol was labeled in the 1-position one would predict that the label of the  $\text{C}_3$ -position should be zero and the label in the  $\text{C}_2$ -position should be the same as in the ethanol, and this is the result that they obtained. Likewise, when converting ethanol labeled in the 2-position the label in carbons in the 1- and 3-positions of the  $\text{C}_3$ -products would be one-half of that of the ethanol; this was in agreement with the experimental results.

The addition of the  $^{14}\text{C}$  alkane shows that it is inert and does not undergo hydrogenolysis. Thus,  $^{14}\text{C}$ -labeled octacosane ( $\text{C}_{28}\text{H}_{58}$ ) was utilized as the reaction solvent for synthesis using a CSTR and it does not produce a detectable amount of either lower or higher molecular weight compounds during more than a week of synthesis [21]. Likewise, the addition of  $^{14}\text{C}$ -labeled  $\text{C}_2$ ,  $\text{C}_3$ ,  $\text{C}_5$  and  $\text{C}_{10}$  alkenes during synthesis did not produce measurable

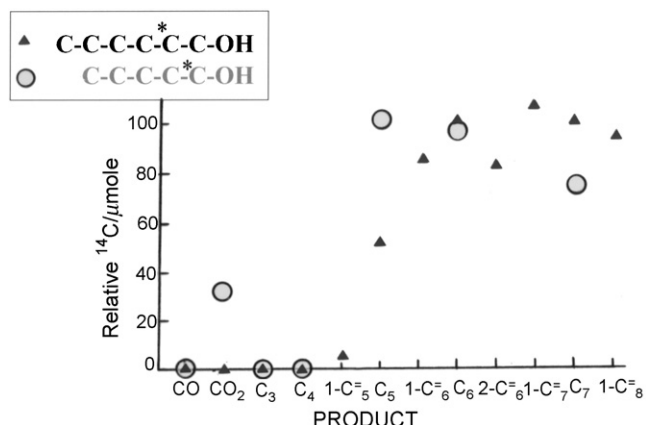
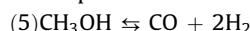


Fig. 7. Radioactivity in the products from FT synthesis when 1- $^{14}\text{C}$ -1-pentanol (○) or 2- $^{14}\text{C}$ -1-hexanol (▲) was added to the synthesis gas.

amounts of lower carbon number compounds expected for the hydrogenolysis reaction even though they did adsorb to initiate chain growth to higher molecular weight compounds. Thus, we conclude that once the hydrocarbon is formed in the presence of syngas it does not undergo hydrogenolysis even though it does chemisorb in a form that allows it to undergo hydrogenation and/or chain growth.

The contribution of the reverse reactions needs to be defined. The early work by Emmett and coworkers [22] employing  $^{14}\text{C}$ -labeled methanol clearly showed that methanol undergoes decomposition under the synthesis reaction conditions:



Thus, when  $^{14}\text{C}$ -labeled methanol is added to the synthesis gas CO a plot of the radioactivity versus carbon number yields a straight line with a slope of one. It is clear that methanol is not stable under synthesis conditions and undergoes the reverse reaction to produce syngas.

For alcohols with carbon number higher than methanol the situation is more complicated. The conversion of these higher carbon number normal alcohols is illustrated by the data of the addition of  $^{14}\text{C}$ -labeled 1-pentanol and 1-hexanol labeled in the carbon 1- and 2-positions, respectively. When the  $^{14}\text{C}$ -1-pentanol was added to the synthesis gas,  $^{14}\text{C}$ -labeled  $\text{CO}_2$  was formed together but the  $\text{C}_1$ – $\text{C}_4$ -products did not have a concentration of  $^{14}\text{C}$  that was high enough to detect (Fig. 7). Furthermore, the label in the CO was also too low to detect. Thus, it is apparent that the carbon in the 1-position of  $^{14}\text{C}$ -1-pentanol was lost as  $\text{CO}_2$ , and not CO as would be expected for the reverse hydroformylation reaction where the alcohol first is dehydrogenated to the aldehyde and then the carbon is extruded as CO. If the carbon was lost from 1-pentanol as CO and the  $\text{CO}_2$  was formed by the water-gas shift reaction, the  $\text{CO}_2$  would have to have had an activity equal to or less than that of the CO, but it could never be greater than that of CO if it was produced by the water-gas shift reaction. The addition of  $^{14}\text{C}$ -labeled  $\text{CO}_2$  has shown that while the reverse water-gas shift reaction does occur, it does not occur to a significant extent. This means that the high radioactivity of the  $\text{CO}_2$  must result from being formed directly as  $\text{CO}_2$  by being extruded from the  $^{14}\text{C}$ -1-pentanol. To place this conclusion on a firmer basis, [2- $^{14}\text{C}$ ]-hexanol was synthesized and added to the synthesis gas fed to the CSTR. With the label in the 2-position, the  $\text{CO}_2$  did not contain a measurable amount of  $^{14}\text{C}$  and a significant amount of  $^{14}\text{C}$ -labeled pentane was formed. This result is taken to mean that as the  $\text{CO}_2$  is being extruded and a hydrogen is added to the  $\text{C}_5$ -hydrocarbon fragment to produce  $n$ -pentane directly from the alcohol. The mechanism for

the expulsion of  $\text{CO}_2$  directly together with the formation of the  $n$ -alkane means that the alcohol has to react with an oxygen source to form a structure that resembles or is an adsorbed carboxylic acid. The data generated to date does not permit one to conclude whether the added oxygen comes from the dissociation of CO, the addition of an OH derived from water, or another source. However, these data are a very strong evidence for at least a mechanism that forms an adsorbed carboxylic acid structure or one that is very similar to it. These data support the conclusions of Blyholder et al. [23] and of Kölbel and Tillmetz [24].

A number of investigators, including our studies, have obtained a negative isotope effect for deuterium for the methanation and the Fischer–Tropsch synthesis. A variety of explanations have been offered to explain these results but as of this date no specific structure has been advanced for the intermediate that could give the negative isotope effect. Thus, this topic will not be covered in this manuscript.

## 6. Structure of the iron catalyst

The early work on catalyst characterization was concerned with iron catalysts used in the high temperature process as practiced, for example, at Sasol. Thus, Dry [25] presented a widely accepted view of the iron catalyst as shown in Fig. 8. At the start of the reaction the catalyst is shown to be predominantly in the form of

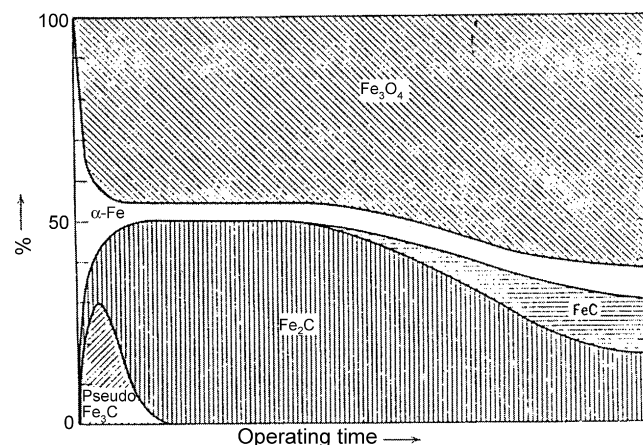


Fig. 8. The changes in the catalyst phases versus time-on-stream during high-temperature FT synthesis with an iron catalyst (from Ref. [25]).

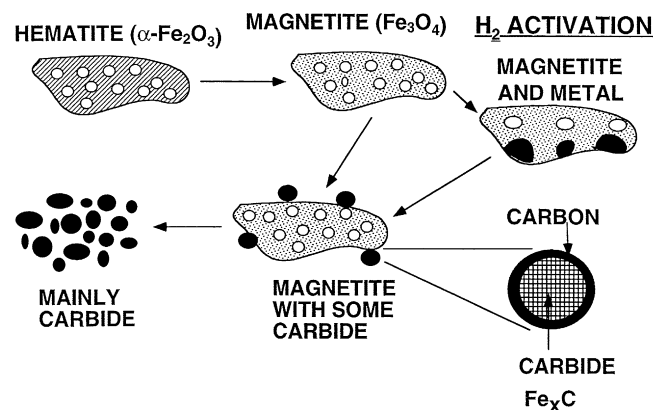


Fig. 9. Schematic representation of the morphological changes that accompany the phase changes that occur on the  $\alpha\text{-Fe}_2\text{O}_3$  catalyst as a result of activation and reaction conditions (from Ref. [26]).

Note: NO COPPER

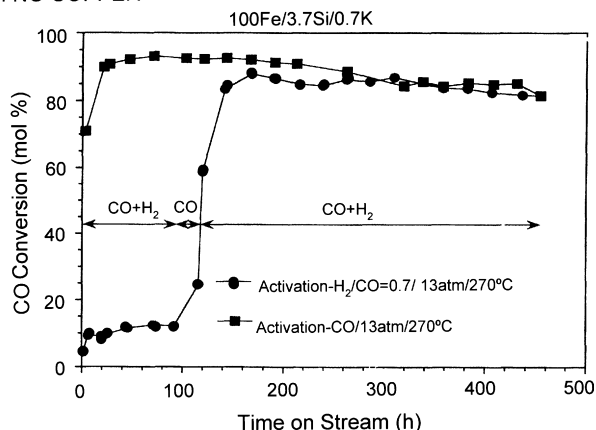


Fig. 10. The CO conversion following activation in CO (■) and in syngas (●) (see text for details).

metallic iron. As the reaction time increases the fraction of metallic iron decreases as it is converted to  $\text{Fe}_3\text{O}_4$  and iron carbides. However, even after a long time-on-stream there is still metallic iron present in the catalyst. It is emphasized that the data in Fig. 8 applies to the low surface area catalyst that is utilized in the high-temperature process [26].

At least two groups have presented similar data for iron catalysts used for the low-temperature process; however, in at least one of these studies the results are based on characterization data obtained for a low surface area catalyst utilized in the La Porte, Texas pilot plant. As depicted in Fig. 9, the large particle is considered to be an iron oxide and the activation converts small nodules on the surface of the large particles to a carbide form which may become dislocated from the surface of the larger particle. This is an attractive model since it could offer an explanation for the difficulties that are found for the separation of wax from iron catalyst. However, the high surface area catalyst does not contain these large particles.

The precipitated iron catalysts have a surface area in the 200–300  $\text{m}^2/\text{g}$  range following calcination at 300–350 °C. These particles, based on the surface area and TEM measurements, are in the size range of 3–6 nm. We find that activation of these catalysts in CO converts 90% or more of the iron oxide to iron carbides; thus, these small realistic iron catalysts do not fit the model shown in Fig. 9. As these catalysts are employed in the FT

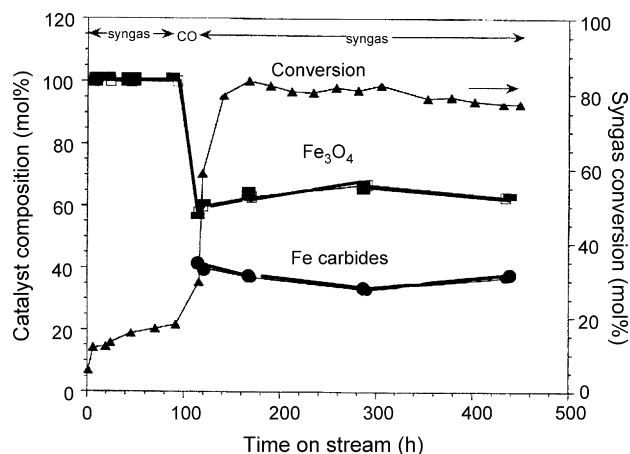


Fig. 11. The phase compositions for an iron catalyst activated first in syngas (up to 100 h on-stream) and then in CO and the CO conversion (▲).

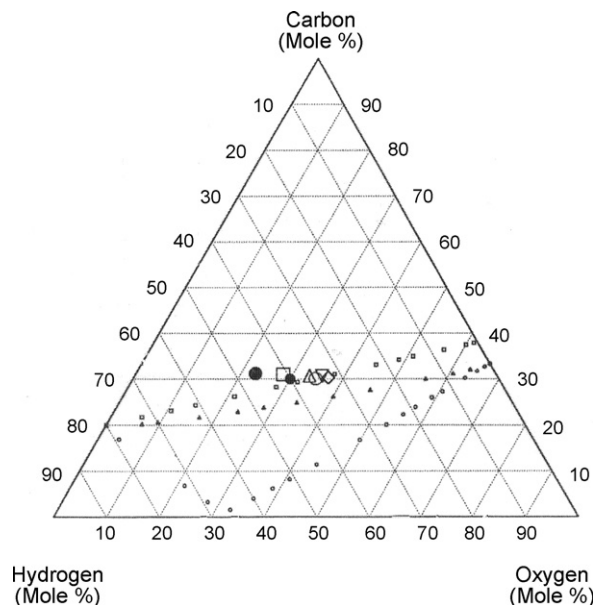


Fig. 12. Calculated phase diagram for iron catalyst exposed to synthesis gas at 300°C (symbols are for the gas composition for increasing CO conversions).

synthesis some of the iron carbide is converted to  $\text{Fe}_3\text{O}_4$  until a steady-state is reached with the amount of carbide in the 40–60% range and will then remain at this level for 2000 h of synthesis. During the early time-on-stream while carbide is being converted to  $\text{Fe}_3\text{O}_4$ , the conversion of CO does not follow the trend line for the loss of carbide; rather the activity shows a common, slow, steady decline during the early period of phase change and during the steady-state of iron carbide/iron oxide.

There has been some debate whether iron oxide has activity for the FT synthesis. The data in Figs. 10 and 11 show that the catalyst, following activation in CO has a high and stable conversion level. On the other hand, the catalyst activated at 270 °C in synthesis gas has a low conversion level that increases slightly with time and then attains a low, stable CO conversion level. After about 100 h on-stream, the syngas flow was terminated and the catalyst was subjected to a flow of pure CO for 24 h. Following the treatment with CO, the system was returned to the normal synthesis conditions, and the catalyst exhibited the same high conversion as the sample initially activated in CO. During these runs small amounts of catalyst samples were withdrawn at increasing time-on-stream. Analysis of the withdrawn samples using Mössbauer spectroscopy showed that the sample following activation and

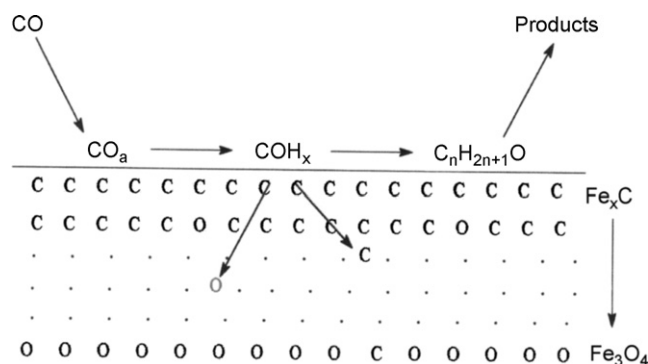


Fig. 13. Schematic of the active low-temperature catalyst during FT synthesis (carbide outer layer with  $\text{Fe}_3\text{O}_4$  inner core).



during the initial period of low CO conversion was essentially  $\text{Fe}_3\text{O}_4$ . Following the 24-h activation in CO, the catalyst contained about 40% of iron carbides and maintained this level during the next 300 h on-stream with the high, stable CO conversion (Fig. 10).

The high temperature thermodynamic data have been extrapolated to the range of the reaction temperature (300 °C). The region that is carbon-rich in Fig. 12 is the region where the iron carbide phase is stable. Below the line defined by the ( $\square$ ) symbols the stable phase is a form of iron oxides. At the low-temperature metallic iron is stable only in essentially a pure hydrogen atmosphere. Also shown in Fig. 12 are symbols defining the compositions at conversion levels of 10–90% CO and these points are located near the line separating the iron carbide and iron oxide phases. Thus, under our reaction conditions we are operating near the region where the sample could be in either the oxide or the carbide phase.

Considering the data from the analysis of many catalyst samples that have been withdrawn during various time-on-stream during the synthesis, we conclude that the conversion of the iron carbide to  $\text{Fe}_3\text{O}_4$  occurs at the middle of the catalyst particle and that the iron oxide core is surrounded by a layer of iron carbides. This is illustrated schematically in Fig. 13 where the lower layers are predominantly iron oxide and the upper layers are nearly forms of iron carbide. It is considered that the catalyst is in a dynamic pseudo-steady-state and the stability of this steady-state depends upon the catalyst composition, the state of the catalyst following the activation period and the reaction conditions [27].

## 7. Conclusions

Considering the reaction data described above, we believe that a reaction mechanism involves an initiation species that differs from the species that is responsible for chain propagation. Because the iron catalyst has water-gas shift activity and our work on water-gas shift catalysis favors a formate mechanism, we propose that the chain initiation species is similar, or the same, as the intermediate in the water-gas-shift reaction. It is, therefore, viewed that an oxygen containing structure that is, or resembles, a formate species can be formed from either CO or  $\text{CO}_2$  and this is responsible for chain initiation (Scheme 7). The species responsible for chain propagation differs from the structure of the chain initiation species and is derived predominantly from CO. It is emphasized that the C–O bond of the initiation species is not broken prior to the addition of the CO to extend the growing chain by one more carbon.

The structure of the high surface area low-temperature iron catalyst is considered to consist of a core of  $\text{Fe}_3\text{O}_4$  that is covered by a layer of iron carbide. The stability of the catalyst is considered to be determined by the ability of the catalyst under the reaction conditions to maintain this layer of iron carbide. There appears to be a synergistic interaction between the alkali promoter and the structural promoter (silica, alumina, etc.) so that the catalyst is more stable when both promoters are present than when either is present alone. This implies that there is a slow continuous replacement of carbon in the iron carbide layer and that a combination of catalyst composition and reaction conditions will define those situations where the iron carbide layer thickness is in a pseudo-equilibrium condition to ensure a very slow catalyst deactivation condition.

## References

- [1] F. Fischer, *The Conversion of Coal into Oils*, (translated by R. Lessing), Ernest Benn Ltd., London, 1925.
- [2] F. Fischer, H. Tropsch, *Brennstoff-Chem.* 7 (1926) 97.
- [3] S.R. Craxford, E.K. Rideal, *J. Chem. Soc.* (1939) 1604.
- [4] P.H. Emmett's class at The Johns Hopkins University, 1965.
- [5] H.H. Podgurski, J.T. Kummer, T.W. DeWitt, P.H. Emmett, *J. Am. Chem. Soc.* 72 (1950) 5382.
- [6] J.T. Kummer, L.C. Browning, P.H. Emmett, *J. Chem. Phys.* 16 (1948) 739.
- [7] H.H. Storch, N. Golumbic, R.B. Anderson, *The Fischer–Tropsch and Related Synthesis*, John Wiley & Sons, New York, 1951.
- [8] D. Gall, E.J. Gibson, C.C. Hale, *J. Appl. Chem.* 2 (1952) 371.
- [9] I. Wender, S. Friedman, W.A. Steiner, R.B. Anderson, *Chem. Ind.* (1958) 1694.
- [10] H. Pichler, H. Schulz, *Chem. Ing. Tech.* 42 (1970) 1162.
- [11] A. Deluzarche, R. Kieffer, A. Muth, *Tetrahedron Lett.* (1977) 3357.
- [12] R.S. Sapienza, M.J. Sansone, L.D. Spaulding, J.F. Lynch, in: M. Tsutsui (Ed.), *Fundamental Research in Homogeneous Catalysis*, vol. 3, Plenum Press, 1979, p. 179.
- [13] R.C. Brady III, R. Pettit, *J. Am. Chem. Soc.* 103 (1981) 1287.
- [14] M. Ritschel, W. Vielstich, *Chem. Ing. Tech.* 52 (1980) 327.
- [15] M. Ritschel, H.-W. Buschmann, W. Vielstich, *Grundlagenforschung zur Fischer–Tropsch-Synthese*, BMFT-FB-T 82-020, January 1982.
- [16] A.T. Bell, *Catal. Rev. Sci. Eng.* 23 (1981) 203.
- [17] S.C. Chuang, Y. Tian, J.G. Goodwin Jr., I. Wender, *J. Catal.* 96 (1985) 396.
- [18] C.J. Wang, J.G. Ekerdt, *J. Catal.* 86 (1984) 239.
- [19] F.A.P. Cavalcanti, D. Blackmond, I. Wender, R. Oukaci, *J. Catal.* 123 (1990) 270.
- [20] B. Shi, B.H. Davis, *Top. Catal.* 26 (2003) 157.
- [21] C.S. Huang, H. Dabbagh, B.H. Davis, *Appl. Catal.* 73 (1991) 237.
- [22] R.J. Kokes, W.K. Hall, P.H. Emmett, *J. Am. Chem. Soc.* 79 (1957) 2069.
- [23] G.D. Blyholder, D. Haihab, W.V. Wyatt, R. Bartlett, *J. Catal.* 43 (1970) 122.
- [24] H. Kölb, K.D. Tillmetz, *Ber. Bunsen.* 76 (1992) 1156.
- [25] M.E. Dry, *Chemtech.* (December) (1982) 744.
- [26] M.D. Shroff, D.S. Kalakkad, K.E. Coulter, S.D. Köhler, M.S. Harrington, M.B. Jackson, A.G. Sault, A.K. Datye, *J. Catal.* 156 (1993) 185.
- [27] Y. Zhang, N. Sirimanathan, R.J. O'Brien, H.H. Hamdeh, B.H. Davis, *Stud. Surf. Catal.* 139 (2001) 125.